The role of vector-baryon channels and resonances in the $\gamma p \to K^0\Sigma^+$ and $\gamma n \to K^0\Sigma^0$ reactions near the $K^*\Lambda$ threshold.

A. Ramos[1] and E. Oset[2]

[1] *Departament d'Estructura i Constituents de la Materia and Institut de Ciencies del Cosmos, Universitat de Barcelona , Martí i Franquès 1, 08028 Barcelona, Spain*

[2] *Departamento de Física Teórica, Universidad de Valencia and IFIC, Centro Mixto Universidad de Valencia-CSIC, Institutos de Investigación de Paterna, Aptdo. 22085, 46071 Valencia, Spain*

(Dated: November 7, 2013)

Abstract

We have studied the $\gamma p \to K^0\Sigma^+$ reaction in the energy region around the $K^*\Lambda$ and $K^*\Sigma$ thresholds, where the CBELSA/TAPS cross section shows a sudden drop and the differential cross section experiences a transition from a forward-peaked distribution to a flat one. Our coupled channel model incorporates the dynamics of the vector meson-baryon interaction which is obtained from the hidden gauge formalism. We find that the cross section in this energy region results from a delicate interference between amplitudes having $K^*\Lambda$ and $K^*\Sigma$ intermediate states. The sharp downfall is dictated by the presence of a nearby N^* resonance produced by our model, a feature that we have employed to predict its properties. We also show results for the complementary $\gamma n \to K^0\Sigma^0$ reaction, the measurement of which would test the mechanism proposed in this work.

PACS numbers: 11.80.Gw, 12.39.Fe, 13.60.-r, 13.75.-n, 14.20.Gk

I. INTRODUCTION

The recent work reported by the CBELSA/TAPS collaboration [1] puts a challenge to the ordinary models of photoproduction of mesons. The reaction is $\gamma p \to K^0\Sigma^+$, which exhibits a peak in the cross section around $\sqrt{s} = 1900$ MeV followed by a fast downfall around $\sqrt{s} = 2000$ MeV. Most remarkable, the differential cross section is flat close to threshold, becomes forward peaked close to the energy where the cross section has a maximum but, up to the resolution of the experiment, appears again isotropic in the region where the total cross section is small and nearly constant, from $\sqrt{s} = 2000$ MeV to $\sqrt{s} = 2200$ MeV. The experiment complements and improves earlier measurements of Crystal Barrel [2] and SAPHIR [3]. As shown in [1], sophisticated models of K photoproduction like K-MAID [4] and SAID [5] grossly fail to reproduce the experimental features, even when changes are made to adapt the models to this particular reaction. The same fate is shown to follow for the models [6–8], as discussed in [3].

In this work we present a theoretical approach that gives an explanation to the features observed in the $\gamma p \to K^0\Sigma^+$ reaction around $\sqrt{s} = 2000$ MeV. The experimental paper [1] hints to some mechanisms involving vector meson-baryon channels, since the prominent feature discussed above occurs in between the $K^*\Lambda$ and $K^*\Sigma$ thresholds, at 2010 MeV and 2087 MeV, respectively. Our model implements the vector-baryon interaction for vectors of the nonet with the octet of baryons obtained in [9], using the local hidden gauge Lagrangians [10–12] and coupled channels in an unitary approach. This vector-baryon interaction leads to the dynamical generation of $1/2^-$ and $3/2^-$ resonances, degenerate in spin-parity, one of which appears around 1970 MeV and couples to ρN, ωN, ϕN but mostly to $K^*\Lambda$ and $K^*\Sigma$. The fact that this resonance appears close to the location of the downfall of the cross section suggests that any realistic theoretical scheme trying to reproduce this problem should consider the explicit incorporation of these channels and their interaction, as done in the present work. We show that the interference of the $K^*\Lambda$ and $K^*\Sigma$ channels, magnified by the presence of the resonance, is essential for reproducing the behavior of the $\gamma p \to K^0\Sigma^+$ cross section around 2000 MeV. We also give predictions for the $\gamma n \to K^0\Sigma^0$ reaction, which has a quite different interference pattern and shows a peak in the energy region where the $\gamma p \to K^0\Sigma^+$ has the downfall. A measurement of the neutral reaction could then bring further light into the physics hidden in these processes.

II. FORMALISM

The hidden gauge approach incorporates automatically vector meson dominance [13], converting the photon into a vector meson, which later on interacts with the other hadrons. Our basic mechanisms for the $\gamma N \to K^*\Sigma$ reaction are depicted in Fig. 1, where we can see the photon conversion into ρ^0, ω, ϕ, followed by the $\rho N, \omega N, \phi N$ interaction leading to the relevant vector-baryon ($V'B'$) channels, which are of $K^*\Lambda$ or $K^*\Sigma$ type, since those are the ones to which the resonance around 1970 MeV couples most strongly according to the model of Ref. [9]. Finally, the intermediate $K^*\Lambda$ or $K^*\Sigma$ states get converted via pion exchange to the final $K^0\Sigma^+$, in the case of γp, or $K^0\Sigma^0$, in the case of γn. We take the vector-baryon amplitudes $VN \to V'B'$ from the work of Ref. [9]. Since in the final state we have a pseudoscalar meson and a baryon, it would be most appropriate to work with a model space that contains both the pseudoscalar-baryon and the vector-baryon channels, as done in [14–16]. Yet, at the energy that we are concerned we can neglect the interaction of the pseudoscalar-baryon channels since they do not produce any resonance around this region [17], and then consider just the interaction of the vector-baryon channels plus the mechanism responsible for the transition from vector-baryon to the final pseudoscalar-baryon that we take from [14]. The formalism of Ref. [9] was developed under the assumption that the

momenta of the external mesons was small. In the present work, the momentum of the photon and, hence, that of the virtual ρ^0, ω or ϕ mesons, is not small, but some of the simplifying assumptions of the model of Ref. [9] are still valid or have a limited influence. On the one hand, neglecting the zeroth component of the polarization vector, ϵ^0, is still possible for these mesons since they acquire the polarization vector of the photon, which is of transverse nature. On the other hand, we have estimated that the size of the linear momentum terms neglected here to be about 15% of the dominant contributions to the $VB \to V'B'$ interaction. This observation can justify a posteriori why the small three-momentum approximation applied in the radiative decays of vector-vector molecules [18–20] led to such good results in spite of the finite momentum of the emitted photons. Further details on the interaction of vectors with mesons and baryons can be seen in the review [21] and in Ref. [22].

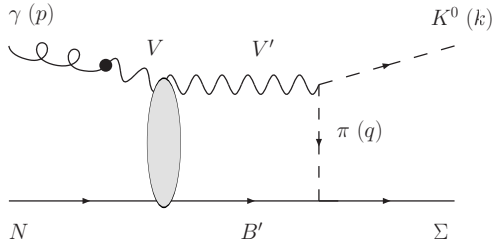

FIG. 1: Mechanism for the photoproduction reaction $\gamma N \to K^0\Sigma$. The symbol V stands for the ρ^0, ω and ϕ mesons, while $V'B'$ denotes the intermediate channel, which can be $K^{*+}\Lambda$, $K^{*+}\Sigma^0$ or $K^{*0}\Sigma^+$, in the case of $\gamma p \to K^0\Sigma^+$, and $K^{*+}\Sigma^-$ or $K^{*0}\Lambda$, in the case of $\gamma n \to K^0\Sigma^0$, the $K^{*0}\Sigma^0$ one not contributing in the later reaction due to the zero value of the $\pi^0\Sigma^0\Sigma^0$ coupling at the Yukawa vertex.

The photon-vector conversion Lagrangian is given by

$$\mathcal{L}_{\gamma V} = -M_V^2 \frac{e}{g} A_\mu \langle V^\mu Q \rangle \ , \tag{1}$$

with $Q = diag(2, -1, -1)/3$ and A_μ being the photon field. The charge of the electron, e, is negative and normalized as $e^2/4\pi = 1/137$.

The $V'PP$ vertex is obtained from

$$\mathcal{L}_{VPP} = -ig\langle [P, \partial_\mu P] V^\mu \rangle \ , \tag{2}$$

with the coupling of the theory given by $g = \frac{M_V}{2f}$ where $f = 93$ MeV is the pion decay constant and M_V the vector-meson mass. The magnitude V_μ is the SU(3) matrix of the vectors of the ρ nonet and P stands for the matrix of the pseudoscalar mesons of the π.

Finally, the Yukawa vertex is described by the Lagrangian:

$$\mathcal{L}_{PBB} = \frac{1}{2}(D+F)\langle \bar{B}\gamma^\mu\gamma^5 u_\mu B\rangle + \frac{1}{2}(D-F)\langle \bar{B}\gamma^\mu\gamma^5 B u_\mu\rangle \ , \tag{3}$$

where the term $\gamma^\mu\gamma^5 u_\mu$ is taken in its non-relativistic form:

$$\gamma^\mu\gamma^5 u_\mu \to \frac{\sqrt{2}}{f}\sigma^i\partial_i\phi \ , \qquad i = 1, 2, 3 \ , \tag{4}$$

B is the matrix representing the baryon octet, and $D = 0.795$, $F = 0.465$ are taken from [**?**].

The amplitude corresponding to the mechanism in Fig. 1 is given by:

$$-it^{\pi-\mathrm{pole}}_{\gamma N\to K^0\Sigma} = e\sum_{V=\rho^0,\omega,\phi}\mathcal{C}_{\gamma V}\sum_{V'B'}t_{VN\to V'B'}\,i\int\frac{d^4q}{(2\pi)^4}\frac{1}{(q+k)^2-M^2_{V'}+i\varepsilon}\frac{1}{q^2-m^2_\pi+i\varepsilon}$$
$$\frac{M_{B'}}{E_{B'}}\frac{1}{P^0-q^0-k^0-E_{B'}(\vec{q}+\vec{k}\,)+i\varepsilon}(\vec{q}-\vec{k}\,)\vec{\epsilon}_\gamma\,\vec{\sigma}\vec{q}\,V_{Y,B'}F(q)\ , \tag{5}$$

where

$$\mathcal{C}_{\gamma V}=\begin{cases}\frac{1}{\sqrt{2}} & \text{for } V=\rho^0\\ \frac{1}{3\sqrt{2}} & \text{for } V=\omega\\ -\frac{1}{3} & \text{for } V=\phi\end{cases}\ , \tag{6}$$

and

$$V_{\Sigma^+,B'}=\begin{cases}\frac{2D}{2f\sqrt{3}} & \text{for } V'B'=K^{*+}\Lambda\\ -\frac{2F}{2f} & \text{for } V'B'=K^{*+}\Sigma^0\\ \frac{2F}{2f}\left(-\frac{1}{\sqrt{2}}\right) & \text{for } V'B'=K^{*0}\Sigma^+\end{cases}\ , \tag{7}$$

in the case of $\gamma p\to K^0\Sigma^+$, while

$$V_{\Sigma^0,B'}=\begin{cases}\frac{2F}{2f} & \text{for } V'B'=K^{*+}\Sigma^-\\ \frac{2D}{2f\sqrt{3}}\left(-\frac{1}{\sqrt{2}}\right) & \text{for } V'B'=K^{*0}\Lambda\end{cases}\ , \tag{8}$$

in the case of $\gamma n\to K^0\Sigma^0$. Note that the factor $-1/\sqrt{2}$ appearing in $V_{Y,B'}$ when $V'=K^{*0}$ accounts for the relation between the neutral meson coupling, $K^{*0}\to\pi^0K^0$, to the charged meson one, $K^{*+}\to\pi^+K^0$, in the $V'PP$ vertex. For the form factor $F(q)$ we take a typical Yukawa static shape, $\Lambda^2/(\Lambda^2+\vec{q}^{\,2})$ with a cut-off $\Lambda=850$ MeV, a value that has been adjusted to reproduce the size of the experimental $\gamma p\to K^0\Sigma^+$ cross section. One could also argue that there can be an extra form factor factor at the meson VPP vertex. In such a case, one should consider our prescription as an empirical way of accounting for these combined finite-size effects.

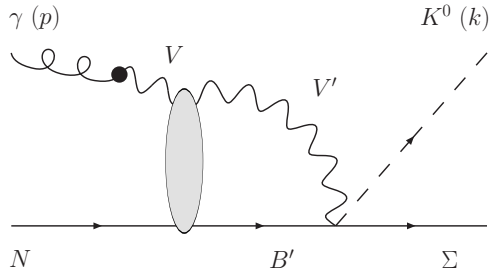

FIG. 2: Kroll-Ruderman contact term to be added to the mechanisms of Fig. 1 to preserve gauge-invariance in the photoproduction reactions $\gamma N\to K^0\Sigma$.

In order to implement gauge invariance, the amplitudes of Eq. (5) must be complemented by the corresponding Kroll-Ruderman contact term [14–16], displayed in Fig. 2 and given by

$$-it^{KR}_{\gamma N\to K^0\Sigma} = e\sum_{V=\rho^0,\omega,\phi}\mathcal{C}_{\gamma V}\sum_{V'B'}t_{VN\to V'B'}\,i\int\frac{d^4q}{(2\pi)^4}\frac{1}{(q+k)^2-M^2_{V'}+i\varepsilon}$$
$$\frac{M_{B'}}{E_{B'}}\frac{1}{P^0-q^0-k^0-E_{B'}(\vec{q}+\vec{k}\,)+i\varepsilon}\,\vec{\sigma}\vec{\epsilon}_\gamma\,V_{Y,B'}\,F(q)\ . \tag{9}$$

After performing the q^0 integration analytically, Eqs. (5) and (9) both develop two structures, $\vec{\sigma}\vec{k}\,\vec{\epsilon}_\gamma\vec{k}$ and $\vec{\sigma}\vec{\epsilon}_\gamma$. Adding all contributions together, we obtain

$$-it_{\gamma N\to K^0\Sigma} = A\vec{\sigma}\vec{k}\,\vec{\epsilon}_\gamma\vec{k} + B\vec{\sigma}\vec{\epsilon}_\gamma \ , \tag{10}$$

where

$$A = e\sum_{V=\rho^0,\omega,\phi}\mathcal{C}_{\gamma V}\sum_{V'B'} t_{VN\to V'B'}\,V_{Y,B'}\,\tilde{G}^{(1)}_{V'B'} \ , \tag{11}$$

and

$$B = e\sum_{V=\rho^0,\omega,\phi}\mathcal{C}_{\gamma V}\sum_{V'B'} t_{VN\to V'B'}\,V_{Y,B'}\,\left(\tilde{G}^{(2)}_{V'B'} + G_{V'B'}\right) \ . \tag{12}$$

The loop functions $\tilde{G}^{(1)}_{V'B'}$, $\tilde{G}^{(2)}_{V'B'}$ and $G_{V'B'}$ are given by

$$\begin{aligned}\tilde{G}^{(1)}_{V'B'} = & \int\frac{d^3q}{(2\pi)^3}\frac{M_{B'}}{E_{B'}}\frac{1}{2\omega_\pi\omega_{V'}}\frac{1}{P^0-E_{B'}-\omega_{V'}+i\varepsilon}\frac{1}{-k^0+\omega_{V'}+\omega_\pi-i\varepsilon} \\ & \frac{1}{P^0-\omega_\pi-k^0-E_{B'}+i\varepsilon}\frac{1}{\omega_\pi+k^0+\omega_{V'}-i\varepsilon}\left[(\omega_{V'}+\omega_\pi)(\omega_{V'}+\omega_\pi-P^0+E_{B'})+k^0\omega_\pi\right] \\ & \times\frac{1}{2\vec{k}^{\,2}}\left\{\frac{3}{\vec{k}^{\,2}}(\vec{q}-\vec{k}\,)\vec{k}\;\vec{q}\,\vec{k}-(\vec{q}-\vec{k}\,)\vec{q}\right\}F(q) \ ,\end{aligned} \tag{13}$$

$$\begin{aligned}\tilde{G}^{(2)}_{V'B'} = & \int\frac{d^3q}{(2\pi)^3}\frac{M_{B'}}{E_{B'}}\frac{1}{2\omega_\pi\omega_{V'}}\frac{1}{P^0-E_{B'}-\omega_{V'}+i\varepsilon}\frac{1}{-k^0+\omega_{V'}+\omega_\pi-i\varepsilon} \\ & \frac{1}{P^0-\omega_\pi-k^0-E_{B'}+i\varepsilon}\frac{1}{\omega_\pi+k^0+\omega_{V'}-i\varepsilon}\left[(\omega_{V'}+\omega_\pi)(\omega_{V'}+\omega_\pi-P^0+E_{B'})+k^0\omega_\pi\right] \\ & \times\frac{1}{2}\left\{(\vec{q}-\vec{k}\,)\vec{q}-\frac{1}{\vec{k}^{\,2}}(\vec{q}-\vec{k}\,)\vec{q}\;\vec{q}\,\vec{k}\right\}F(q) \ ,\end{aligned} \tag{14}$$

and

$$G_{V'B'} = \int\frac{d^3q}{(2\pi)^3}\frac{M_{B'}}{E_{B'}}\frac{1}{2\omega_{V'}}\frac{1}{P^0-E_{B'}-\omega_{V'}+i\varepsilon}\,F(q) \ . \tag{15}$$

with

$$P^0=\sqrt{s};\quad \omega_\pi=\sqrt{\vec{q}^{\,2}+m_\pi^2};\quad \omega_{V'}=\sqrt{(\vec{q}+\vec{k}\,)^2+m_{V'}^2};\quad E_{B'}=\sqrt{(\vec{q}+\vec{k}\,)^2+M_{B'}^2} \ . \tag{16}$$

We note that the only factor that can produce a pole in the integrand of the former loop functions is $(P^0-E_{B'}-\omega_{V'}+i\varepsilon)^{-1}$ when P^0 matches the energy of an intermediate $V'B'$ state, where $V'=K^*$ and $B'=\Lambda$ or Σ. In order to account for the width of the K^* vector meson, we replace $i\varepsilon$ in this factor by $i\Gamma/2$, with $\Gamma=50.5$ MeV.

The cross section for the $\gamma N\to K^0\Sigma$ reactions, obtained after summing over final spins and averaging over polarizations, including in this way the contributions of $1/2^-$ and $3/2^-$ states, is given by:

$$\frac{d\sigma_{\gamma N\to K^0\Sigma}}{d\Omega} = \frac{1}{16\pi^2}\frac{M_N M_\Sigma}{s}\frac{k}{p}\,\overline{\sum}\sum\mid t_{\gamma N\to K^0\Sigma}\mid^2 \ , \tag{17}$$

where

$$\overline{\sum}\sum\mid t_{\gamma N\to K^0\Sigma}\mid^2 = \frac{1}{2}\left\{\left[\mid A\mid^2\vec{k}^{\,2}+2\,\mathrm{Re}\,(AB^*)\right]\vec{k}^{\,2}\,\sin^2\theta+2\mid B\mid^2\right\} \ . \tag{18}$$

It is obvious from the previous expression that the cross section obtained with this model produces an angular distribution which is symmetrical with respect to 90^o and will not reproduce the forward-peaked cross section around $\sqrt{s} = 2000$ MeV reported in the experiment [1]. Two mechanisms were suggested there to play this role: the nucleon-pole term in the s-channel and the $\gamma p \to K^0\Sigma^+$ transition being mediated by K^* exchange in a t-channel configuration. This second option involves an anomalous VVP coupling, which is proportional to the relatively large photon momentum and can contribute to the $VB \to V'B'$ transition in the problem considered here. Yet, the term contains a $\vec{\sigma}$ operator from the PBB vertex and does not interfere with the spin-independent transition mediated by vector-meson exchange. Consequently, even if these anomalous contributions might not be negligible in the present problem, they would mostly go to a background part that would not spoil the essential mechanism for the downfall of the cross section advocated here. As for implementing a nucleon-pole term, we note that one should take other resonance contributions as well, especially those that are close to the energy region of interest. Given this uncertainty, we have opted for not adding any supplementary contribution to our model, with the aim of investigating whether our vector-baryon coupled channel formalism, which implicitly incorporates the effect of dynamically generated resonances, contains the basic mechanisms that provide a qualitative explanation of the experimental observations.

III. RESULTS

We start this section by checking if the interference effect pointed out in Ref. [24] for the differences between the $\gamma p \to \eta p$ and $\gamma n \to \eta n$ cross sections in the region of the $K\Lambda, K\Sigma$ thresholds is also important in the $\gamma N \to K^0\Sigma$ reactions explored in the present work. The authors of Ref. [24] found a destructive interference between the $K^+\Lambda$ and $K^+\Sigma^0$ states excited by the photon in the $\gamma p \to \eta p$ reaction. Since the $K^+\Lambda$ is not present in the neutral $\gamma n \to \eta n$ reaction, this cancellation is absent there, explaining in this way the enhanced neutral cross section over the charged one. Analogously, in the $\gamma N \to K^0\Sigma$ reactions studied here, the photon couples to both the $K^{*+}\Lambda$ and the $K^{*+}\Sigma^0$ states in the $\gamma p \to K^0\Sigma^+$ process, but only to the $K^{*+}\Sigma^-$ state in the case of $\gamma n \to K^0\Sigma^0$. This can be easily checked from the sum of the direct photon couplings to the ρ^0, ω and ϕ mesons, which implicitly buils up the appropriate couplings of the photon to charged vector mesons. However, the situation is slightly more involved in the present work because the amplitude $t_{VN\to V'B'}$, involving rescattering, may induce transitions to states containing a neutral K^* meson, such as $K^{*0}\Sigma^+$ in the $\gamma p \to K^0\Sigma^+$ reaction and $K^{*0}\Lambda$ in the $\gamma n \to K^0\Sigma^0$ one (the intermediate $K^{*0}\Sigma^0$ state does not contribute in the latter case because of the zero value of the $\pi^0\Sigma^0\Sigma^0$ coupling at the Yukawa vertex). As already discussed in the formalism, we are interested in the region of the $K^*\Lambda$ threshold, where the anomaly has been seen, and we only consider K^*Y states in the intermediate $V'B'$ channels. In Fig. 3 we see how the consideration of the different intermediate channels, $K^*\Sigma$ (dashed lines) and $K^*\Lambda$ (dotted lines), build up the final cross section (solid lines), in the case of the $\gamma p \to K^0\Sigma^+$ (upper panel) and $\gamma n \to K^0\Sigma^0$ (lower panel) reactions. As in the work of Ref. [24], we can appreciate in Fig. 3 the tremendous effect of interferences. The destructive interference between the $K^*\Sigma$ and $K^*\Lambda$ amplitudes, of similar size and shape in the case of the $\gamma p \to K^0\Sigma^+$ reaction, produce an abrupt downfall of the cross section right at the position of the resonance generated by the VB interaction model. In contrast, in the case of the $\gamma n \to K^0\Sigma^0$ reaction, the $K^*\Sigma$ and $K^*\Lambda$ amplitudes are quite different, giving rise to a final cross section retains the peak at the position of the resonance to a large extent. In addition, the interference becomes constructive in between the $K^*\Lambda$ and $K^*\Sigma$ thresholds, which slows down the decrease of the neutral cross section at higher energies.

We next compare the obtained cross section for the $\gamma p \to K^0\Sigma^+$ reaction (solid line) with the

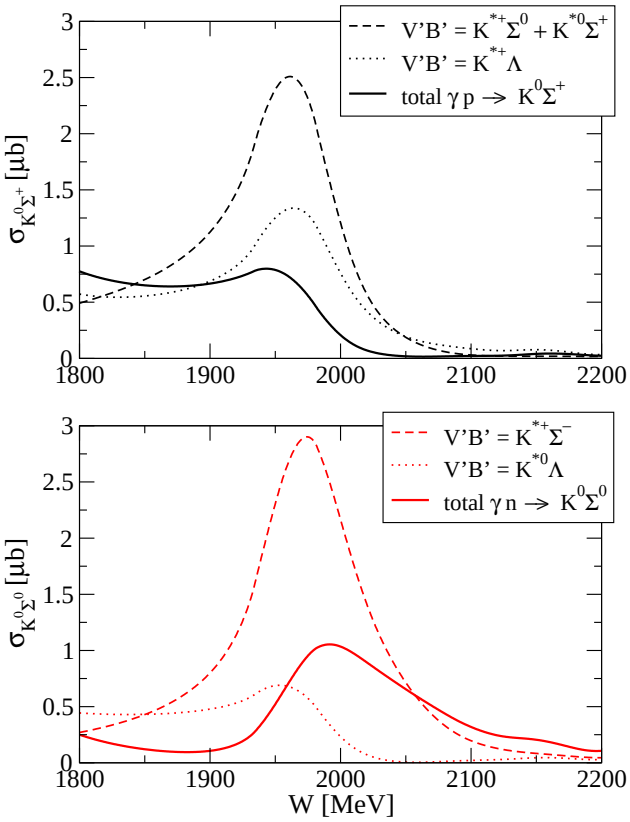

FIG. 3: Contributions to the $\gamma p \to K^0\Sigma^+$ (upper panel) and $\gamma n \to K^0\Sigma^0$ (lower panel) cross sections.

experimental data [1] in the upper panel of Fig. 4. Note that, as in the experiment, the results in this figure and in all the other ones presented in this work, have been averaged over the photon energy in bins of ± 50 MeV width. We also recall that our model does not intend to obtain a quantitative agreement over the complete energy region. In fact, the behavior at lower $\sqrt{s}$ is not well reproduced. The data has the tendency to decrease as we lower the energy towards the threshold of the reaction, while our model shows an enhancement close to $\sqrt{s} = 1700$ MeV. This is due to the fact that the employed VB coupled-channel interaction model [9] produces a narrow resonance at 1700 MeV, coupling strongly to ρN and sizably to $K^*\Lambda$. However, experimentally one finds a much wider $3/2^-$ resonance [26]. In fact, to reproduce the width of this resonance, which lies below the lowest threshold of the VB coupled-channel interaction model employed here, it should be necessary to incorporate, additionally to ρN, lower-lying pseudoscalar-baryon states, such as πN in D-wave and $\pi\Delta$, as done recently in [27]. However, the incorporation of the $K\Lambda$, $K\Sigma$ channels in the study of the resonance around 2000 MeV has minor effects, as can be seen in Fig. 6 of [14]. In view of that, we focus only on interpreting the behavior of the $\gamma p \to K^0\Sigma^+$ reaction around the region of the $K^*\Lambda$ threshold.

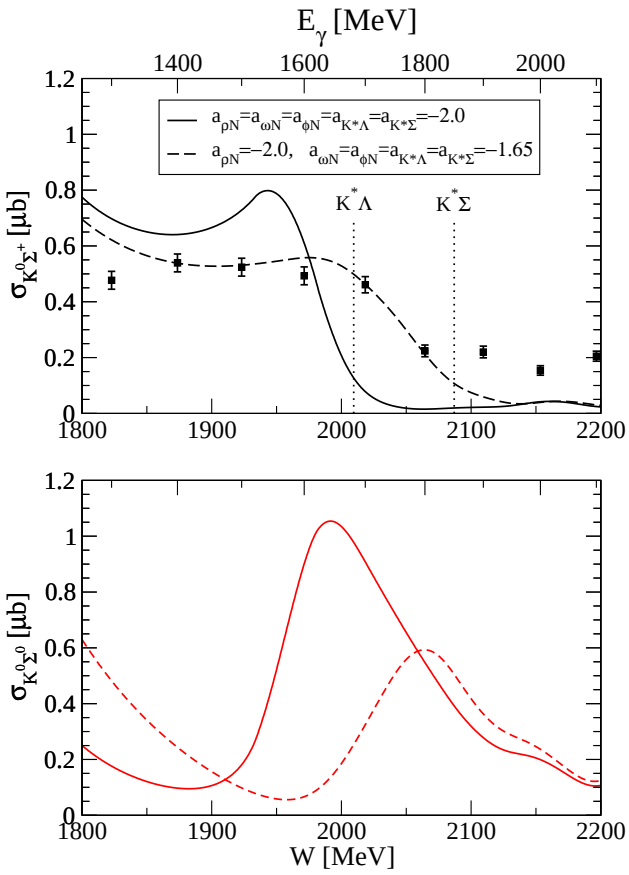

FIG. 4: Upper panel: Comparison of the $\gamma p \to K^0\Sigma^+$ cross section, obtained with two parameter sets, with the CBELSA/TAPS data of Ref. [1]. The downfall of the cross section allows one to redefine the parameters of the model and give a better prediction for the position of the resonance. Lower panel: Predictions for the $\gamma n \to K^0\Sigma^0$ cross section using two parameter sets.

We observe that the downfall of the theoretical results displayed by the solid line appears 60 MeV below the energy at which the experimental cross section presents the abrupt drop. Actually, since this downfall is sensitive to the position of the resonance produced in this energy region, we can fine tune the parameters of the model using the CBELSA/TAPS data, and obtain in this way a more realistic prediction of the resonance mass. We recall that the vector-baryon interaction model employed [9] depends on the subtraction constants a_l ($l = \rho N$, ωN, ϕN, $K^*\Lambda$ and $K^*\Sigma$), used to regularize the meson-baryon loop function at a regularization scale of $\mu = 630$ MeV, that were taken to be have the natural size value of -2, as determined in [28]. By changing the subtraction constants to a value of -1.65, except $a_{\rho N}$ which is kept at its original value of -2, we obtain the dashed curve in Fig. 4, which shows the downfall at the energy where the experimental cross section presents a sudden drop. This is quite an achievement of the employed VB coupled-channel interaction, which explains this behavior from an interference effect between various resonant amplitudes involving intermediate $K^*\Lambda$ and $K^*\Sigma$ channels, a feature that none of the isobar phenomenological models, using K-matrix coupled-channel methods [4–8] but ignoring K^*Y channels, is able to obtain. Our model could be further tested with a measurement of the neutral $\gamma n \to K^0\Sigma^0$ cross section, a prediction of which is shown in the lower panel of Fig. 4 for the two different parameter sets employed here.

We can now obtain the characteristics of the resonance around the energy region of the $K^*\Lambda$

threshold obtained with the new parameter set. We recall that, in the original model where all the subtraction constants were set to -2 [9], the resonance was found to be represented by a pole in the second Riemann sheet, as defined e.g. in [25], at $z = 1977 + \mathrm{i}53$ MeV. It was also pointed out there that, in a coupled channel model with mesons having a mass distribution, like ρ and K^* in our case, there is a fuzzy description of the VB thresholds involving either one of these mesons. When a resonance appears close to one of such thresholds, finding the pole can be a complicated task. For this reason, in these cases, the resonance properties were also derived from the shape of the amplitudes in the real energy axis [9]. In the case of the resonance discussed here, the real axis method produced a resonance mass of $M_R = 1972$ MeV and a width of $\Gamma_R = 64$ MeV. Changing all the subtraction constants to -1.65, except $a_{\rho N}$ which is kept to its original value of -2, the new resonance properties are $M_R = 2035$ MeV and $\Gamma_R = 125$ MeV. With the new parameter set the resonance appears 60 MeV up in energy, lying now above the $K^*\Lambda$ threshold to which it couples substantially and, consequently, being almost twice wider. It is interesting to note that two resonances of negative parity around this region of energy, $N^*(2080)(3/2^-)$ and $N^*(2090)(1/2^-)$, which appeared in earlier versions of the PDG, have been eliminated in the latest version [26]. A resonance with these quantum numbers in that energy region, albeit with some uncertainty in the precise position, is unavoidable in our model due to the attractive character and strength of the vector-baryon interaction [9]. These states also appear in a different work that uses the same vector-baryon channels, together with the pseudoscalar-baryon ones and a somewhat different dynamics [29]. Experimental support for a $(3/2^-)$ resonance around 2080 MeV has been found recently from an analysis of SPring 8 LEPS data on the $\gamma p \to K^+\Lambda(1520)$ reaction in [30]. Our results provide another solid backing for the existence of an odd parity resonance around this energy region.

Finally, the calculated differential cross section of the $\gamma p \to K^0\Sigma^+$ reaction is compared with the recent experimental CBELSA/TAPS data in Fig. 5. The differential cross section is given as a function of the kaon center-of-mass angle for several bins of the laboratory photon energy having a width of ± 50 MeV. The corresponding central center-of-mass $W \equiv \sqrt{s}$ energies are also quoted in the various panels. We already noted that our model predicts a symmetrical angular distribution around 90^o, which is obvious from the structure of Eq. (17). In order to obtain a better agreement with the forward-peaked data, one would have to extend the model with P-wave contributions, not-necessarily resonant, that would interfere constructively at forward angles and destructively at backward ones. The interesting thing to realize is that our VB coupled channel model builds up some angular structure with increasing energy, which becomes weaker above the energy where the cross section experiences the downfall, as can be better quantified by the ratio of the difference over the sum of the calculated cross section at 0^o and 90^o given in Table I.

W (MeV)	1823	1874	1923	1971	2018	2064	2109	2153	2197
$\frac{\sigma(0^o)-\sigma(90^o)}{\sigma(0^o)+\sigma(90^o)}$	0.14	0.20	0.24	0.29	0.31	0.30	0.23	0.17	0.16

TABLE I: Ratio of the difference over the sum of the calculated $\gamma p \to K^0\Sigma^+$ cross section at 0^o and 90^o.

IV. SUMMARY AND CONCLUSIONS

This work has presented a theoretical study of the $\gamma p \to K^0\Sigma^+$ reaction around $\sqrt{s} = 2000$ MeV, where the cross section shows a rapid downfall and the differential cross section changes from being forward-peaked to being essentially flat. The fact that these features occur between the $K^*\Lambda$ and $K^*\Sigma$ thresholds hints at the plausible explanation that these channels are crucial ingredients in

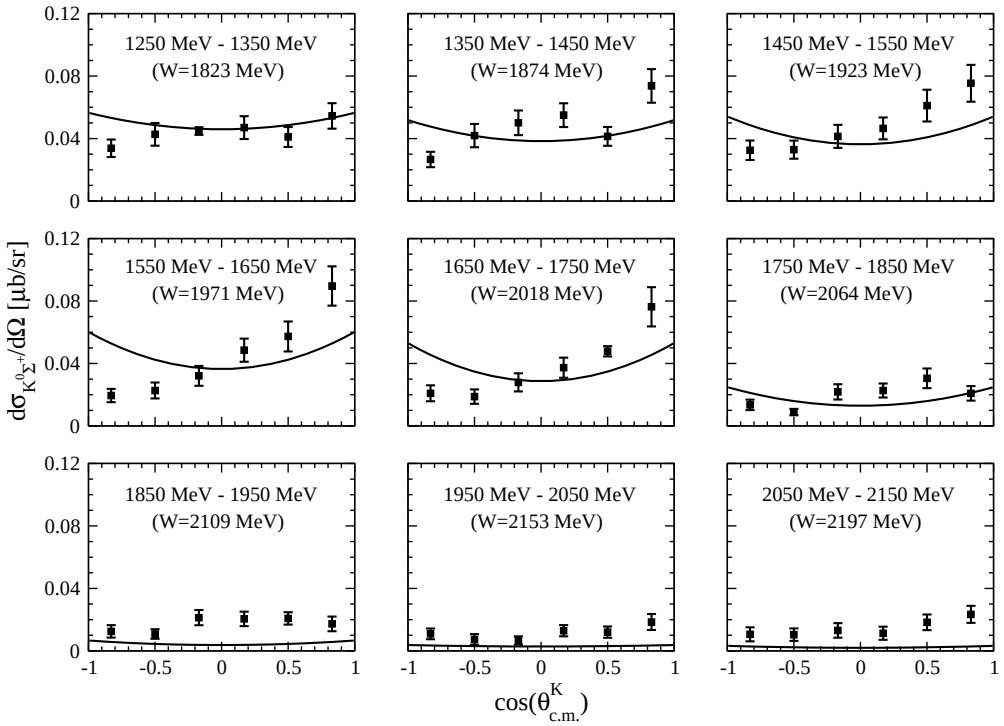

FIG. 5: Differential cross section for the $\gamma p \to K^0\Sigma^+$ reaction as a function of the kaon center-of-mass angle, for several bins of the laboratory photon energy.

any theoretical model trying to reproduce the data in this energy region. In fact, none of the existing K-matrix coupled-channel resonance models that ignore these channels is able to provide a satisfactory explanation of the observed structures.

We have developed a model for this reaction that incorporates the interaction between vector mesons of the nonet with baryons of the octet, obtained from local hidden gauge Lagrangians and implementing unitarization in coupled channels. This vector-baryon interaction produces a resonance in the energy region of interest that couples strongly to $K^*\Lambda$ and $K^*\Sigma$ states.

Our results for the $\gamma p \to K^0\Sigma^+$ reaction show indeed a rapid drop of the cross section, which is a consequence of a delicate interference between amplitudes containing $K^*\Lambda$ and $K^*\Sigma$ intermediate states, magnified by the presence of a resonance that our model produces in this energy region. These interferences are present in the $\gamma n \to K^0\Sigma^0$ reaction, also studied in this work, although their different balance produces a neutral cross section that has a maximum where the charged reaction presents the sudden drop. Since this structure is sensitive to the position of the resonance, we have used the CBELSA/TAPS data to fine tune the parameters of our model and obtain in this way a more realistic prediction of the resonance mass, that we now find at 2030 MeV, in the energy region where earlier versions of the PDG pointed out the presence of two close resonances with spin-parity $1/2^-$ and $3/2^-$. The important role played by a resonant $N^*(2080)$ contribution has also been pointed out recently from an analysis of SPring8 LEPS $K^+\Lambda(1520)$ photoproduction data. A measurement of the interesting signature that this resonance leaves on the $\gamma n \to K^0\Sigma^0$ reaction, showing a peak structure where the $\gamma p \to K^0\Sigma^+$ reaction has a sharp downfall, would give extra support to the existence of this state.

We have also obtained the $\gamma p \to K^0\Sigma^+$ differential cross sections and have observed the tran-

sition to a weaker angular distribution above the energy where the cross section experiences the downfall, as in experiment.

The model presented here is by no means a complete one. Explicit background contributions and genuine resonant terms would have to be included to reproduce the complete set of data, from the $K^0\Sigma$ threshold up to the energy region explored here. However, this study has brought up the important observation that the consideration of the $K^*\Lambda$ and $K^*\Sigma$ states in a unitary coupled-channel scheme is crucial to reproduce the rapid downfall of the $\gamma p \to K^0\Sigma^+$ cross section around 2000 MeV. This hypothesis would be further tested by a measurement of the neutral reaction $\gamma n \to K^0\Sigma^0$, which can bring further light into the physics hidden in these processes.

Acknowledgments

This work is partly supported by the Spanish Ministerio de Economia y Competitividad and European FEDER funds under the contract numbers FIS2011-28853-C02-01 and FIS2011-24154, by the Generalitat Valenciana in the program Prometeo 2009/090, and by Grant No. 2009SGR-1289 from the Generalitat de Catalunya. We also acknowledge the support of the Consolider Ingenio 2010 Programme CPAN CSD2007-00042 and of the European Community-Research Infrastructure Integrating Activity Study of Strongly Interacting Matter (acronym HadronPhysics3, Grant Agreement n. 283286) under the Seventh Framework Programme of EU.

[1] R. Ewald, B. Bantes, O. Bartholomy, D. Bayadilov, R. Beck, Y. A. Beloglazov, K. T. Brinkmann and V. Crede *et al.*, Phys. Lett. B **713**, 180 (2012) [arXiv:1112.0811 [nucl-ex]].
[2] R. Castelijns *et al.* [CBELSA/TAPS Collaboration], Eur. Phys. J. A **35**, 39 (2008) [nucl-ex/0702033].
[3] R. Lawall, J. Barth, C. Bennhold, K. -H. Glander, S. Goers, J. Hannappel, N. Joepen and F. Klein *et al.*, Eur. Phys. J. A **24**, 275 (2005) [nucl-ex/0504014].
[4] http://www.kph.uni-mainz.de/MAID/(version 29.3.2007).
[5] R. A. Arndt, et al. http://gwdac.phys.gwu.edu.
[6] A. V. Anisovich, A. Sarantsev, O. Bartholomy, E. Klempt, V. A. Nikonov and U. Thoma, Eur. Phys. J. A **25**, 427 (2005) [hep-ex/0506010].
[7] A. V. Sarantsev, V. A. Nikonov, A. V. Anisovich, E. Klempt and U. Thoma, Eur. Phys. J. A **25**, 441 (2005) [hep-ex/0506011].
[8] A. Usov and O. Scholten, Phys. Rev. C **72**, 025205 (2005) [nucl-th/0503013].
[9] E. Oset, A. Ramos, Eur. Phys. J. **A44**, 445-454 (2010) [arXiv:0905.0973 [hep-ph]].
[10] M. Bando, T. Kugo, S. Uehara, K. Yamawaki and T. Yanagida, Phys. Rev. Lett. **54**, 1215 (1985).
[11] M. Bando, T. Kugo and K. Yamawaki, Phys. Rept. **164**, 217 (1988).
[12] U. G. Meissner, Phys. Rept. **161**, 213 (1988).
[13] J. J. Sakurai, Currents and Mesons (University of Chicago Press, Chicago, 1969).
[14] E. J. Garzon and E. Oset, Eur. Phys. J. A **48**, 5 (2012) [arXiv:1201.3756 [hep-ph]].
[15] K. P. Khemchandani, A. Martinez Torres, H. Kaneko, H. Nagahiro and A. Hosaka, Phys. Rev. D **84**, 094018 (2011) [arXiv:1107.0574 [nucl-th]].
[16] K. P. Khemchandani, A. Martinez Torres, H. Nagahiro and A. Hosaka, Phys. Rev. D **85**, 114020 (2012) [arXiv:1203.6711 [nucl-th]].
[17] T. Inoue, E. Oset and M. J. Vicente Vacas, Phys. Rev. C **65**, 035204 (2002) [hep-ph/0110333].
[18] R. Molina, D. Nicmorus and E. Oset, Phys. Rev. D **78**, 114018 (2008) [arXiv:0809.2233 [hep-ph]].
[19] H. Nagahiro, J. Yamagata-Sekihara, E. Oset, S. Hirenzaki and R. Molina, Phys. Rev. D **79**, 114023 (2009) [arXiv:0809.3717 [hep-ph]].
[20] T. Branz, L. S. Geng and E. Oset, Phys. Rev. D **81**, 054037 (2010) [arXiv:0911.0206 [hep-ph]].
[21] E. Oset, A. Ramos, E. J. Garzon, R. Molina, L. Tolos, C. W. Xiao, J. J. Wu and B. S. Zou, Int. J. Mod. Phys. E **21**, 1230011 (2012) [arXiv:1210.3738 [nucl-th]].

[22] H. Nagahiro, L. Roca, A. Hosaka and E. Oset, Phys. Rev. D **79**, 014015 (2009) [arXiv:0809.0943 [hep-ph]].
[23] B. Borasoy, Phys. Rev. D **59**, 054021 (1999) [hep-ph/9811411].
[24] M. Doring and K. Nakayama, Phys. Lett. B **683**, 145 (2010) [arXiv:0909.3538 [nucl-th]].
[25] L. Roca, E. Oset and J. Singh, Phys. Rev. D **72**, 014002 (2005) [hep-ph/0503273].
[26] J. Beringer *et al.* [Particle Data Group Collaboration], Phys. Rev. D **86** (2012) 010001.
[27] E. J. Garzon, J. J. Xie and E. Oset, Phys. Rev. C **87**, 055204 (2013) arXiv:1302.1295 [hep-ph].
[28] J. A. Oller and U. G. Meissner, Phys. Lett. B **500** (2001) 263 [hep-ph/0011146].
[29] D. Gamermann, C. Garcia-Recio, J. Nieves and L. L. Salcedo, Phys. Rev. D **84**, 056017 (2011) [arXiv:1104.2737 [hep-ph]].
[30] J. -J. Xie and J. Nieves, Phys. Rev. C **82**, 045205 (2010) [arXiv:1007.3141 [nucl-th]].